

# **Imaging the rupture process and postseismic deformation of the 2019 Ridgecrest earthquake sequence with high-resolution geodetic data**

Kang Wang (kangwang@berkeley.edu) and Roland Bürgmann  
*Berkeley Seismology Lab, UC Berkeley*

The 2019 Ridgecrest earthquake sequence was the most recent major seismic event to occur in the continental US, and its surface deformation was particularly well imaged by a dense network of Global Navigation Satellite System (GNSS) stations and several satellite radar interferometry (InSAR) missions. Combined with seismic recordings, these high-resolution surface deformation measurements provided essential constraints on the rupture process and slip distribution of the 2019 Ridgecrest earthquake sequence, including the triggering relationship between the Mw 6.4 foreshock on July 4 and the Mw 7.1 mainshock 34 hours later, and the distribution of slip on the fault as a function of depth. However, we show that the published coseismic slip models of the 2019 Ridgecrest earthquake sequence exhibit large variations, despite the good coverage of both geodetic and seismic observations. This highlights the true uncertainties of the routinely performed earthquake rupture inversions and challenges the interpretation for underlying rupture processes. The 2019 Ridgecrest earthquake sequence also caused significant postseismic transient deformation in the surrounding areas. We find that at least three mechanisms, including afterslip, poroelastic rebound and viscoelastic rebound, are required to explain the postseismic deformation observed by InSAR and GNSS  $\sim 2.5$  years after the mainshock. Specifically, the near-to-medium field postseismic GNSS and InSAR displacements are consistent with afterslip and poroelastic rebound, while the far-field GNSS data are best explained by viscoelastic relaxation in the upper mantle. In particular, the pattern of observed vertical displacement in the near field is overall opposite to what the afterslip model predicts, but consistent with the model of poroelastic rebound. The observed postseismic deformation due to poroelastic rebound also allows us to probe the hydrological properties of the shallow crust. We show that the Sentinel-1 LOS displacement time series from the ascending track 64 and GNSS time series at sites close to the mainshock epicenter are consistent with poroelastic rebound models with a hydrological diffusivity of  $\sim 0.1 \text{ m}^2/\text{s}$  in the top 2km.

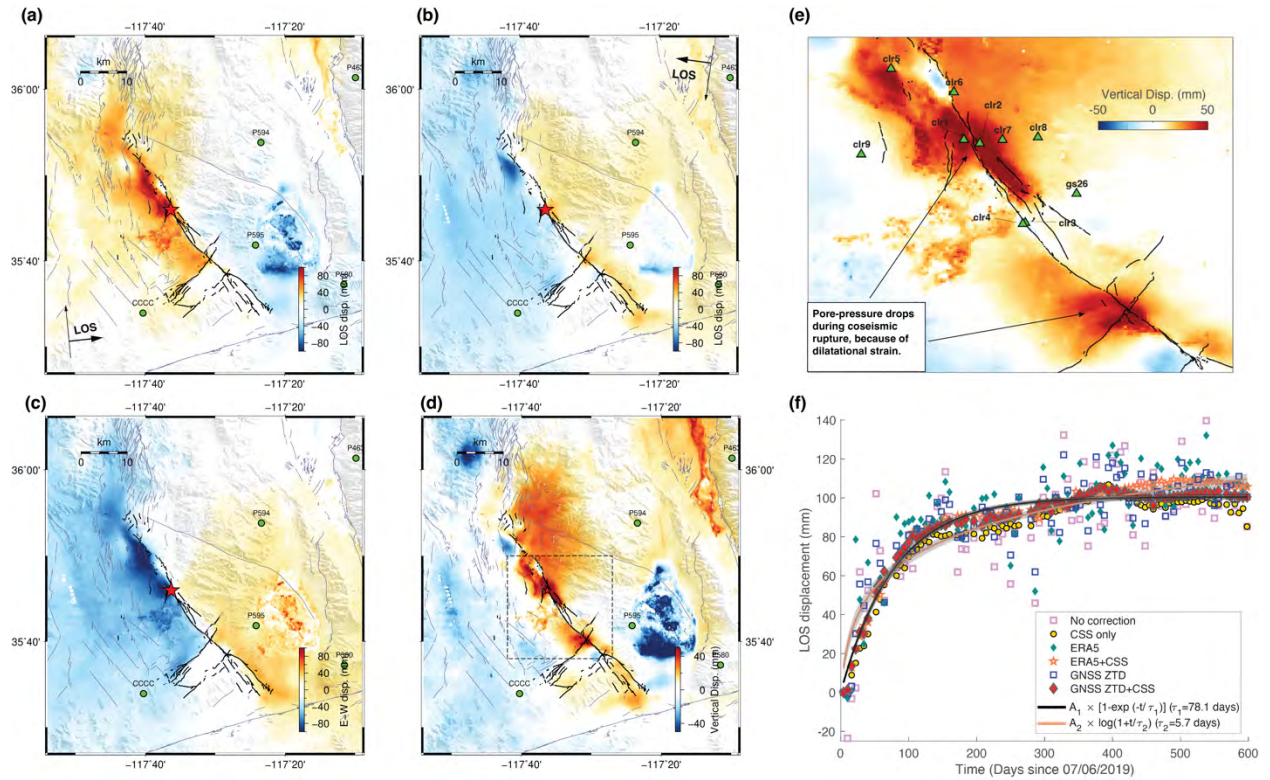


Figure 1. Sentinel-1 InSAR observations of postseismic deformation following the 2019 Ridgecrest earthquake sequence. (a) and (b) cumulative line-of-sight (LOS) displacements 2 years after the mainshock derived from Sentinel-1 data of the ascending track ASC64, and descending track D071, respectively. (c) and (d) show the cumulative postseismic displacements along the East-West and Vertical directions, respectively, by decomposing the LOS displacements from both the ascending and descending tracks. (e) Zoom-in of the vertical component of postseismic InSAR observations near the fault complexities. (f) example LOS time series from the ascending track ASC64 at a point near the mainshock epicenter obtained with different methods to correct for the atmospheric noise.

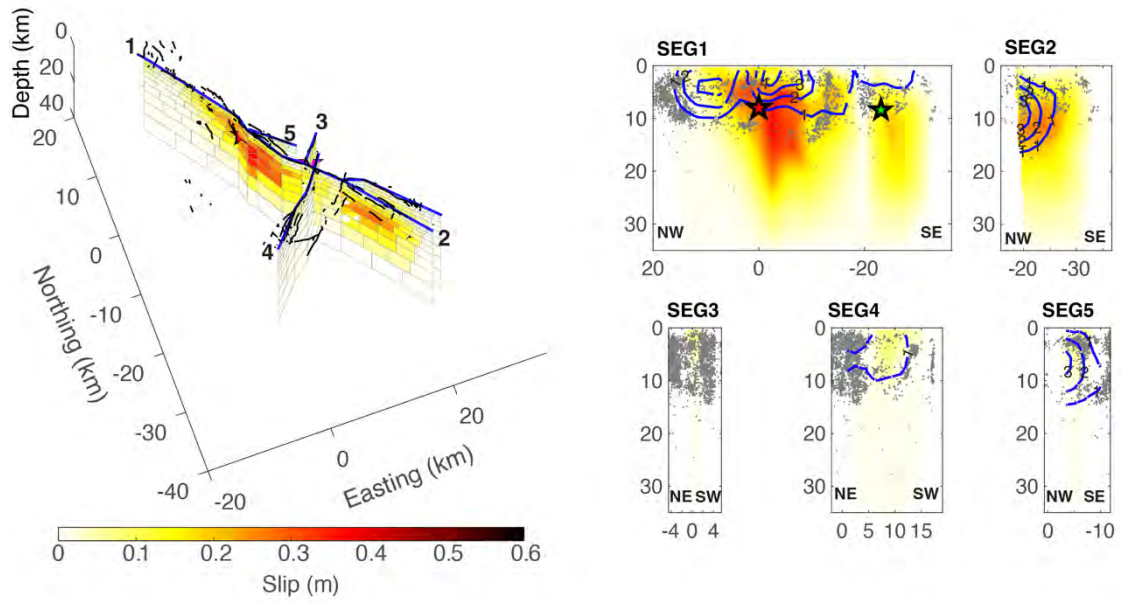


Figure 2. Distribution of cumulative afterslip  $\sim 2.0$  years after the mainshock. Grey dots in panels to the right represent the aftershocks during  $\sim 2$  weeks after the mainshock (Shelly, 2019). Blue contours represent the coseismic slip contours at 1-meter interval (from Wang et al., 2020). Red star represents the hypocenter of the mainshock. Green star denotes the approximate location of the Mw 5.5 aftershock on 06/30/2020.